Creation Research Society Quarterly 2024 60:300–320

Lithification of Sediments

Part II: Field Study in the Great Falls Coal Field, Montana

Peter Klevberg and Michael J. Oard

Abstract

Recent research has produced data useful in inferring burial depths for sandstones from compaction microtextures. Burial depths can also be inferred from erosional remnants and coal rank, among other means. These methods are especially useful over generally horizontal plains when other methods are unavailable to provide minimum overburden depths. That immense amounts of erosion occurred in the study area has long been recognized, but no effective lithification model has been available whereby to estimate burial depths or diagenetic environments. In this paper, we present research from the northern Great Plains focused on sandstones in an effort to develop a semi-quantitative lithification model for estimating initial overburden thickness (burial depth) and conditions of lithification. While development of such a model eludes us, approximations are possible and can be very helpful in studying Earth history.

Key Words: burial depth, coal rank, intergranular volume, Great Falls Coal Field, lithification, porosity, sandstone

Introduction

There are many wide plains across the Earth to which continental erosion studies do not apply, which are devoid of coal, adequate erosional remnants or folds, etc., by which to estimate depths of sediments eroded from the landscape. The Great Plains of North America form such a location, with much of the Great Plains devoid of coal for inferring burial depth. In these locations, an estimate of the erosion can be attempted using the character of sandstones at or near the surface. For this method to provide us with confidence, it needs to be checked against other methods. We have previously analyzed the variables involved in sandstone cementation (Klevberg and Oard, 2023). The objective of this project was to attempt to find a correlation between burial depth of sandstones and coals and their lithologic properties. The location of the study area is shown in Figure 1. Non-geologists may benefit

Accepted for publication May 23, 2023

from the primer on lithification in Appendix A.

Geologic Setting

The study area is suited to the objectives of the project due to its structural simplicity, well-developed stratigraphy, the lithologies present, and nearby erosional remnants. It is located on the western edge of the Northern Plains within sight of the Rocky Mountains. The mountain front is abrupt, with significant deformation of sedimentary strata to the west and little deformation to the east of the Disturbed Belt in northwestern Montana. While nearly level sedimentary strata characterize the landscape east of the Disturbed Belt, there is some apparent deformation. The Sweetgrass Arch (Figure 1) is the dominant structure in the area. It is an antiform trending north-northwest to south-southeast from just southeast of Great Falls to near the Canadian border. The limbs dip only a few degrees below the horizontal to the west and east.

Figure 1. Outline of Montana showing study area (rectangle). Anticline symbol marks the trend of Sweetgrass Arch, the primary structural feature impacting the study area.

Planation surfaces, erosion surfaces capped with coarse gravel, typify the area. Relict valleys containing the Missouri River and its tributaries cut into these surfaces, and erosional remnants (buttes) project from them (Figures 2 and 5). Lower benches are smaller and more dissected; the Greenfields Bench (a.k.a. Fairfield Bench) is the largest intact remnant of a planation surface in the study area. The gravel cap is composed of lithologies found in the Rocky Mountains to the southwest. Based on the clast size and slope, and the lateral extent and architecture of the deposits, the gravel was catastrophically deposited. These gravel-capped erosion surfaces are characteristic of north-central Montana. The geologic map (Vuke et al., 2002) describes them simply as "terrace gravels" since they mantle terraces, which in this case are portions of a planation surface. Had these terraces formed over long periods of time by fluvial erosion, a weathering gradient would be expected in the gravel that caps them, but this is not observed. In interpreting these features, it therefore appears more likely that First, Second, and Third Benches (Figure 2) are fractal features that could be expected to result from waning sheet flow or nascent channelized flow during the transition from the Abative Phase to Dispersive Phase of the Deluge (Walker, 1994; Klevberg and Oard, 1998; Oard and Klevberg, 1998; Barrick, 2018, pp. 95–102; Barrick et al., 2020).

Both the plains and the nearby mountains are dominated by sedimentary rocks. The Front Range is largely steeply dipping limestone and dolostone strata with interbedded clastics, while the rocks of the plains are largely clastics with a slight westward dip (west limb of Sweetgrass Arch). The Greenfields Bench is an eastward-dipping planation surface carved into westward-dipping strata (Figure 8), carved indiscriminately into hard and soft rocks and mantled with gravel. This is typical of planation surfaces, which are not being created by modern processes but rather destroyed by them (Oard, 2008, 2013). Evidence of glaciation, in the form of diamict (drift, till), is found north of the Greenfield Bench, and a relict (outwash) channel forms the north boundary of the bench and possibly marks the southern extent of continental glaciation. The apparent extent of glaciation is irregular but approximately covered the northernmost fifth of the study area.

Sedimentary strata are commonly interpreted as transgressive-regressive cycles that resulted in deposition of primarily marine strata with some interbedded continental (non-marine) materials (Carstarphen et al., 2011). Carbonates are much more common at greater depth, and nearer the surface, bentonite and other volcaniclastic materials predominate. The most common rocks are fine-grained clastics. Igneous rocks in the study area are most notably shonkonite flows of the Adel Mountains Volcanics that cap Square Butte and other nearby buttes south of the Sun River and west of the Missouri River (Figure 2). Laccoliths, dikes, and sills are common in the Highwood Mountains and

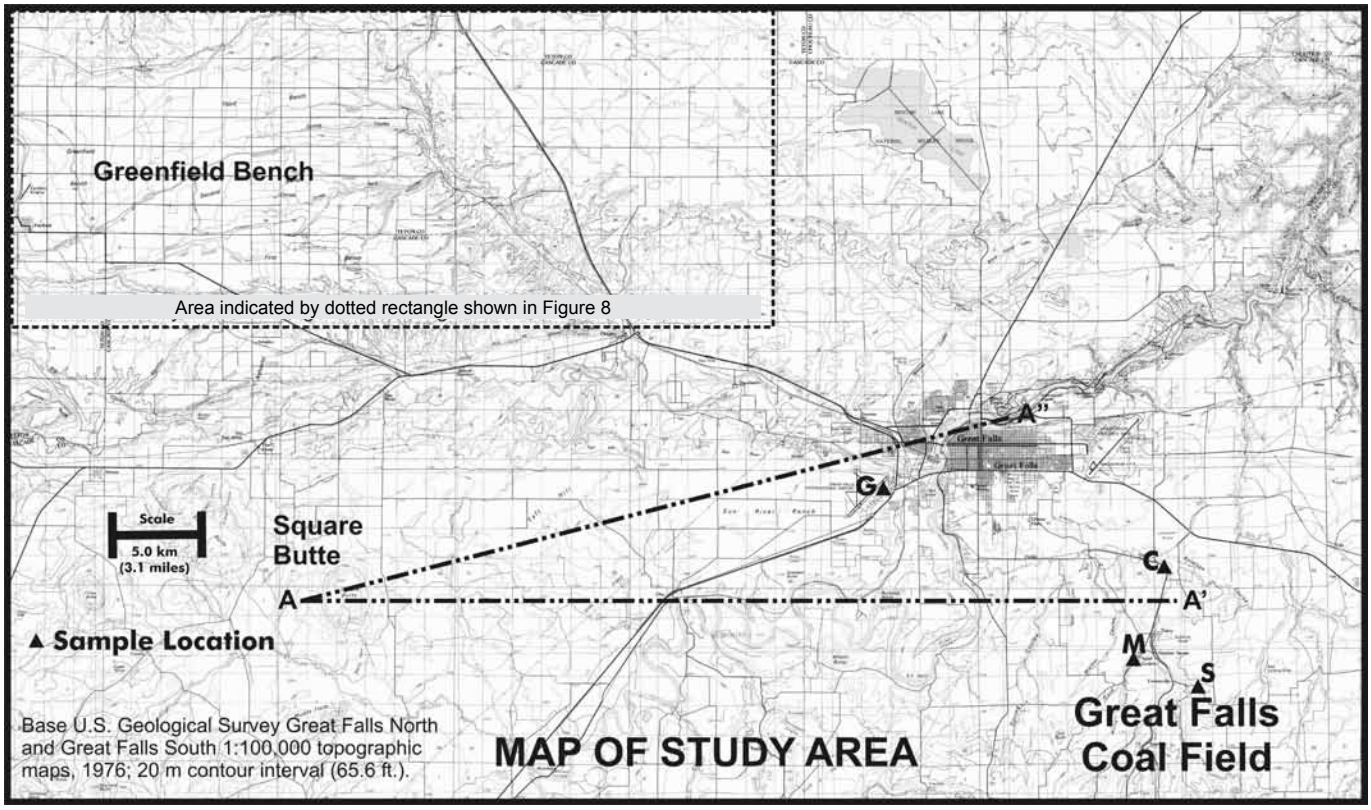

Figure 2. Location of study area is shown on Figure 1. Line A-A' is the cross-section shown on Figure 6, and Figure 7 is the section indicated by the line A-A"

Little Belt Mountains east and southeast, respectively, of the study area. Pediments from these mountains ramp down into the benches on the plains. As much as 2,500 m (8,000 ft.) of sedimentary rocks overlie metamorphic basement in the study area (Carstarphen et al., 2011).

Stratigraphy and Structure

Bedrock is exposed as outcrops along the valley sides (Figure 2) but is mantled by soil cover or diamict where not capped by gravel on benches. Most of the formations and distinctions between their members must be determined from subcrop (borehole data). The dominant lithologies are shale and claystone. Lesser amounts of sandstone, siltstone, and bentonite are encountered. Limestone is minor, and conglomerate is uncommon. The principal sandstones are found in the Flood Member of the Blackleaf Formation (Montana Group), the Sunburst Sandstone, and Cut Bank Sandstone members of the Kootenai Formation, and the uppermost Morrison Formation (Colorado Group). The stratigraphy is presented on the idealized section in Figure 9 and in greater detail in Appendix C. Figures 6 and 7 show both stratigraphy and structure.

Coal

Coal is present in the Blackleaf, Kootenai, and Morrison Formations (Vuke, 2000). The coal of commercial value has been variously classified as basal Kootenai or upper Morrison; the original distinctions in these formations was made based on assumed evolutionary age and not on lithologic grounds (Fisher, 1909). Later, the Kootenai came to be recognized by area drillers as the first red bed, and the first major coal became the marker for the upper Morrison. The Morrison coal extends east approximately 100 miles (170 km) from the Great Falls mining district to Lewistown (Figure 1) and to the west 25 miles (40 km) and was mined at various locations along this length where topography afforded access. The main coal seams in the study area are overlain by approximately 55 m (150 to 200 ft.) of overburden and were accessed from the valley walls near the mining communities of Tracy, Sand Coulee, Centerville, and Stockett (labeled "Great Falls Coal Field" on Figure 2). Mining was by room-and-pillar methods with horse-drawn cars. Mining ceased shortly after

World War II (Vuke, 2000). While the coal is of good quality for heat production, its high sulfur content (up to 4%) and competition from nearby petroleum production has prevented redevelopment of the resource (Silverman and Harris, 1967; Rossillon et al., 2009).

Methodology

This section describes sample collection and analysis and the means of estimating overburden thickness and compaction. The geologic setting is described in the following section.

Sampling

Four samples were collected by the lead author in or near the Great Falls Coal Field: one from the basal member (Flood) of the Blackleaf Formation (G), and three from the subjacent Kootenai Formation: Sunburst Member (S) near the top of the formation, Cut Bank Member from near the base (C), and a sample from the sandstone at the contact between the Kootenai and Morrison Formations (M). The locations of these samples are shown on the map of Figure 2. Sample G was collected from a run of core (Figure 3), sample C from a fresh road cut, and samples M and S from outcrops. Hand samples were fresh, sound rock.

Analysis

The samples were submitted to American Engineering Testing's petrology laboratory in Saint Paul, Minnesota. The laboratory prepared thin sections and reported on the properties of the samples (Appendix B). The samples were classified per Folk (1974) as shown in Table I and Figure 4.

Estimating Overburden

Five methods for estimating burial depth were outlined in Part I (Klevberg and Oard, 2023). These are: 1) from the height of erosional remnants, 2) projected from an eroded anticline or dome, 3) from coal rank, 4) from the amount of continental margin sediments, and 5) from stratigraphy. The first, third, and fifth methods are applicable here.

Height of erosional remnants is a useful measure in the study area. Particularly prominent is Square Butte (Figure 5), west of Great Falls (Figure 2). If the shonkonite capping Square Butte was emplaced as a flow, then about 365 m (1,200 ft.) of sediments were removed from above the samples collected for this project. As shown in Figures 6 and 7, the sedimentary strata that appear level and uniform to the eye are actually dipping to the southwest and vary in thickness. If the strata were deposited before uplift (i.e., original horizontality), then some of these contacts may make a better datum to compare the thickness of overlying strata than simply using elevation above modern sea level. We compared both, interpolating and rounding.

Coal in the Great Falls Coal Field is sub-bituminous B and high volatile bituminous C (Anderson, n.d.; Fisher, 1909; Silverman and Harris, 1967; Rossillon et al., 2009). Charts or curves for estimating burial depth (e.g., Thomas, 2013) assume the present average geothermal gradient to correlate the temperature for pyrolysis of kerogen to coal with depth of burial.

Stratigraphic estimates are more problematic. Outcrop information is primarily from the coal field and major valleys. Subcrop information is primarily from water wells and a couple of wildcat oil wells; this information was obtained from the Ground Water Information Center of the Montana Bureau of Mines and Geology. Published information was consulted for the study area (Figure 8). Figure 9 was created from well logs and Carstarphen et al., (2011). The four samples collected for this project were from the south end or west limb of the Sweetgrass Arch (described in a following section), while Figure 9 is from the west limb approximately 30 miles (50 km) northwest of the sampling locations. The nearly horizontal attitude of the beds and their general uniformity does not appear to introduce any large errors into the correlation. The vertical locations of the samples are indicated on the composite log. A complete composite log for Cascade and Teton Counties is provided in Carstarphen et al. (2011); this was used to create the separate rock column and stratigraphic column shown on Figure 10. As is evident from the large amount of white space in the right column, much of the alleged time has no rock identified with it. Some of these unconformities are likely true unconformities (erosional surfaces), such as the unconformity on top of the Belt Supergroup, while others are paraconformities representing imaginary (inferred) time. The true unconformities represent material that was eroded before additional material was deposited. Thus, the rock column represents *minimum* overburden. However, if some of the stratigraphic column was never deposited above the four sample locations due to nondeposition, lateral thinning of formations, etc., then it is possible that the stratigraphic method will overestimate the original burial depth.

Estimating Compaction

The method of estimating compaction of sandstones is described in Bjørlykke (2014). Sandstone properties used for these estimates are shown in Table II.

1. Intergranular volume is based only on size of framework grains and is 49% for fine-grained sandstone (Chuhan et al., 2002). We give them all an initial porosity (η_0) of 49%.
2. All are poorly cemented, so assume no significant void loss due to quartz cement.
3. Grain shape: high grain angularity produces higher porosity (Fawad et al., 2011). Reduce 4% for angular-

Figure 3. Lead author logging core from boring in basal (Flood Member) Blackleaf Formation sandstone. Sample G was obtained from slightly more than 9 m (30 ft.) into the sandstone bedrock.

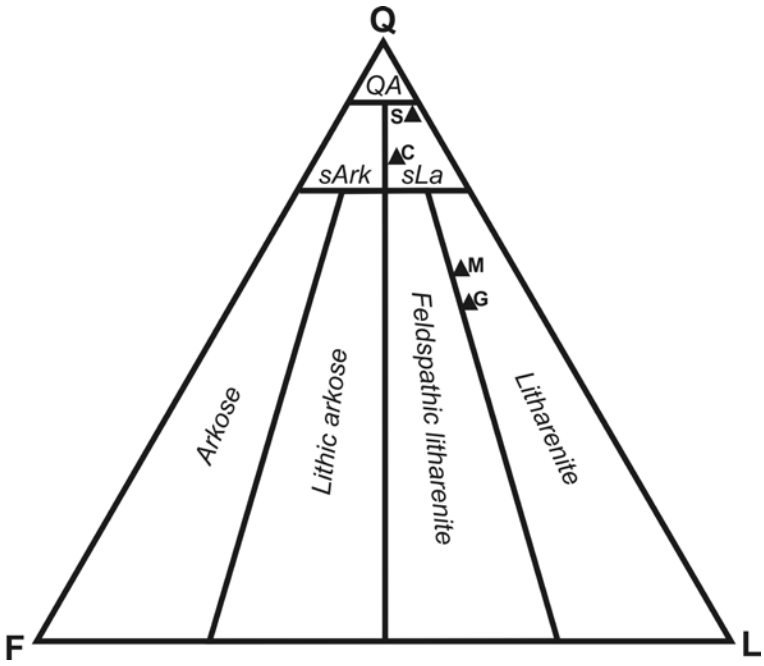

Figure 4. The four sandstone samples plotted on the Folk (1974) ternary diagram.

Table I. Sandstone Classification

Properties	G008C	G008G	G008M	G008S
Quartz	75–85%	55–60%	60–65%	85–90%
Feldspars	3–5%	5–10%	5–10%	1–2%
Lithic Fragments	10–15%	30–35%	25–30%	10–15%
Matrix	cryptocrystalline	cryptocrystalline	cryptocrystalline	cryptocrystalline
Cement (in addition to matrix)	poorly cemented, minor calcite	poorly cemented, minor calcite	poorly cemented, iron oxide, minor quartz	poorly cemented, minor iron oxide
Classification	submature to mature fine-grained sublitharenite	immature to sub-mature fine-grained litharenite	immature to submature fine-grained litharenite	immature fine-grained sublitharenite
Sampling Locations				
Latitude	47°29'05.85"	47°23'08.16"	47°26'46.12"	47°23'57.44"
Longitude	111°21'08.16"	111°07'27.49"	111°08'57.14"	111°10'09.59"

Figure 5. Square Butte, an erosional remnant rising 330 m (1,100 ft.) above the plains west of Great Falls, Montana. It is capped by the hard igneous rock shonkonite, which protects the softer sedimentary rocks beneath it. The similar Crown Butte is several miles in the background.

grain-dominated sandstone and zero for well-rounded.

4. Sorting: the greater the degree of sorting, the greater the porosity, but fracturing with depth decreases sorting (i.e., increases heterogeneity or grading) as fragments are generated. Estimated range of porosity change from poorly sorted to well-sorted to be 6%.
5. Matrix content: the greater the amount of clay and other grains, the lower the remaining porosity. We assumed half of filled pores are cement, so the rest would be initial matrix. Matrix+cement value provided by laboratory.
6. Water compaction: estimate the compaction factor due to water would be one-half the difference of dry sand and wet sand (measured on dry basis). Based on lead author's experience with engineered fills, well-sorted sands would be an approximately 5% decrease, and poorly sorted sands, 9%.

Table III shows the authors' estimates of η_0 using the above factors (#2 = no change).

Comparing With Coal Rank

The sandstone estimates shown above are considerably higher than the eroded

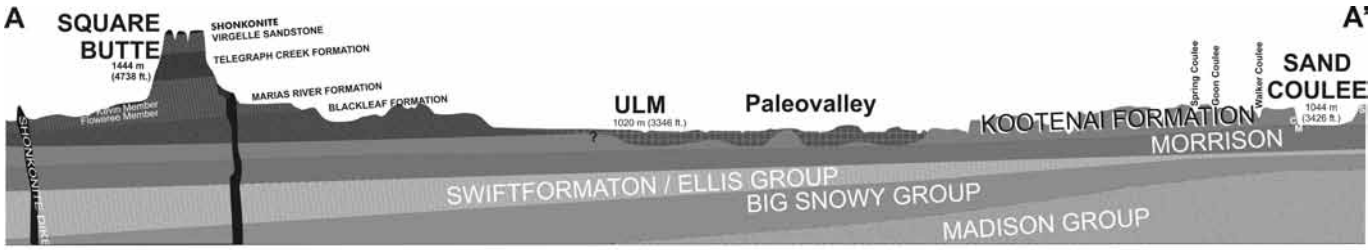

Figure 6. Geologic cross section derived primarily from Vuke (2000) following line A-A' on Figure 2.

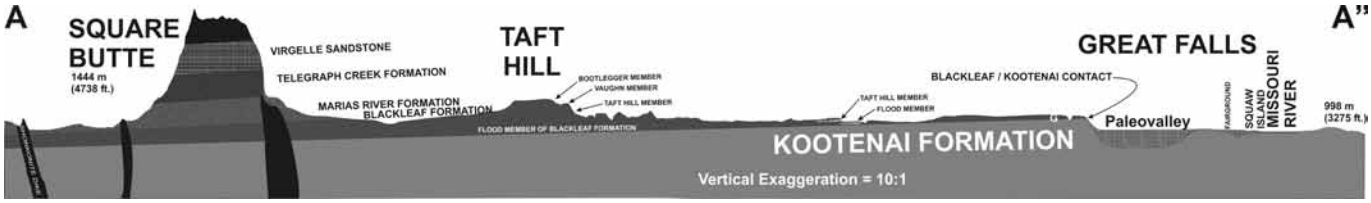

Figure 7. Geologic cross section derived from Vuke (2000) and Vuke et al. (2002) following line A-A" on Figure 2.

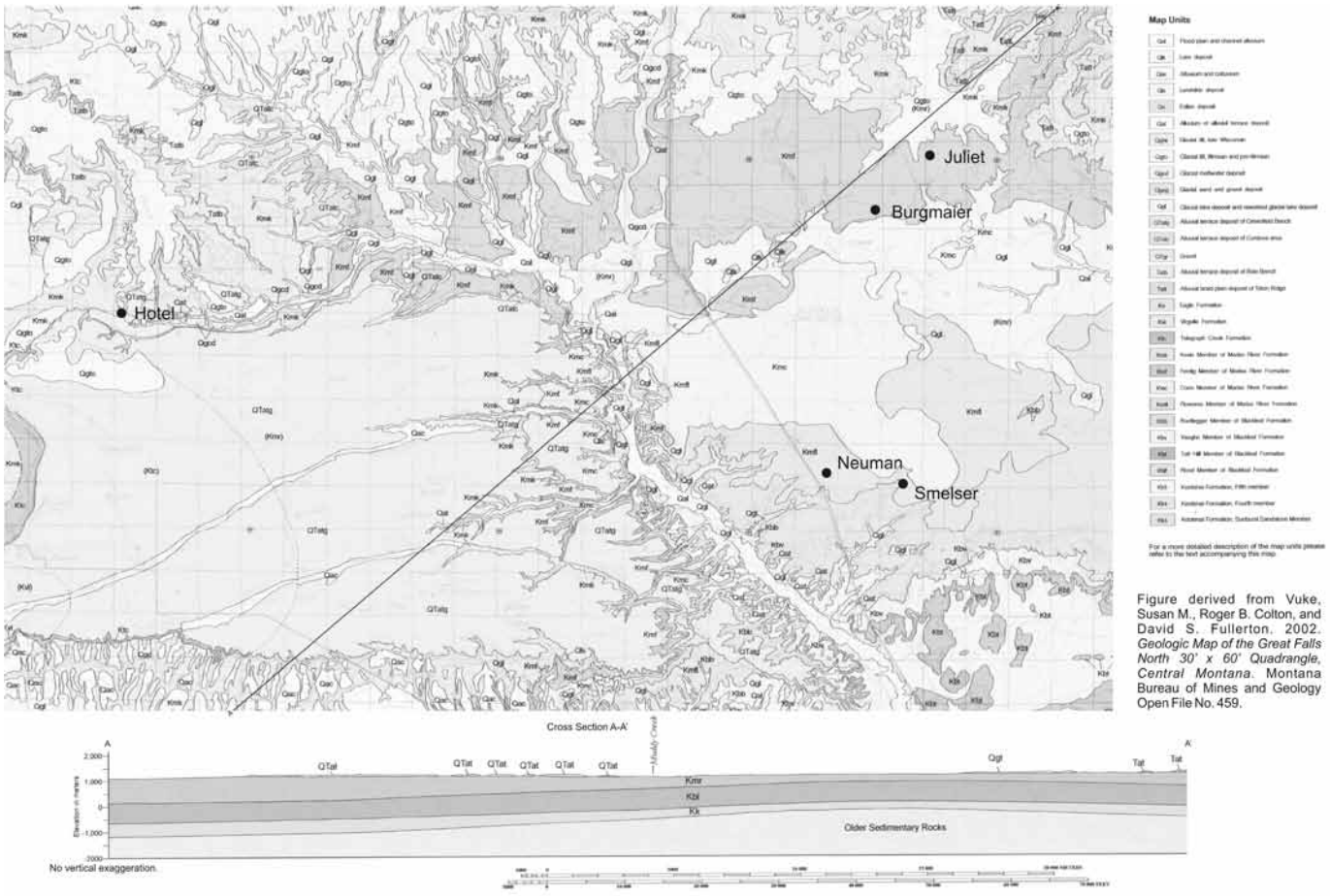

Figure 8. Geologic map with cross section showing Greenfields Bench, from Vuke et al. (2002), showing locations of well logs used in Figure 9.

overburden estimates based on coal rank. We do not know why there is such a large difference, but it could be due to further assumptions in the results of Bjørlykke (2014). Typical petroleum basin modeling incorporates uniformitarian, deep-time assumptions (Klevberg, 2022). Bjørlykke (2014), however, points out that time is not an important factor in sandstone compaction. Based on the rank of the coal and assuming a geothermal gradient of 26–27°C/1,000 m (i.e., increase of 15°F per 1,000 ft. of depth), this coal was buried about 2,800–4,000 m (9,180–13,120 ft.) (Thomas, 2013).

Groundwater Modeling

We had originally proposed to use Aqtesolv® software to model groundwater flow through unconsolidated sediment and gradually consolidating sediment under the assumption that groundwater transport of silica either upward or laterally into the sand strata would have been a particularly important means of lithifying sandstones. As described in Part I of this paper (Klevberg and Oard, 2023), this now seems unlikely, and recent research has not supported this hypothesis (Bjørlykke and Jahren, 2018; Prajapati et al., 2020). Therefore, the transport modeling idea was dropped.

Findings

Two sandstone samples were classified as litharenites, and two as sublitharenites (Table I). Properties observed in thin section are summarized in Table II. The detailed laboratory report is contained in Braaten and Moulzolf, 2018 (Appendix B). Figures 11 through 14 show hand samples, cut and lapped samples, and thin-section magnified images.

Samples of coal were not collected as part of this project; coal sampling and analysis was done by the U.S. Bureau of Mines in previous decades. The coal ranges from sub-bituminous B to high-volatile bituminous C with a

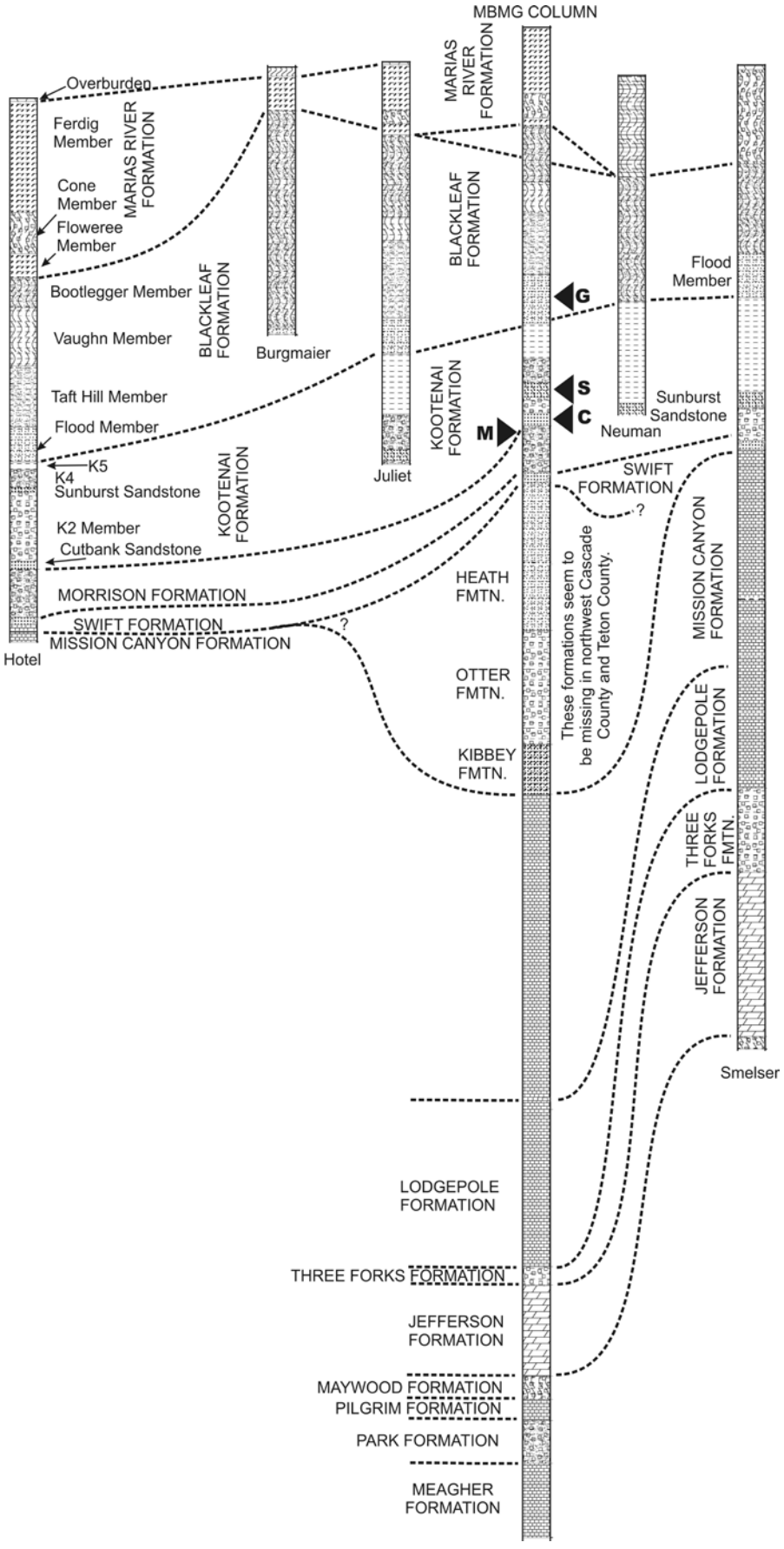

Figure 9 (*left*). Stratigraphic section showing formations encountered per five available well logs and the composite (MBMG) column from Carstarphen et al. (2011), as shown in Figure 8. Stratigraphic position of the four sandstone samples collected for this project shown by <.

heating value of 9,000 to 13,000 Btu/lb.[1] (Silverman and Harris, 1967). Enough samples from enough locations were collected to provide considerable precision in representing an enormous mass of coal. Silverman and Harris (1967, p. iv) state: "The Great Falls–Lewistown coal field contains an estimated 750 million short tons of bituminous and subbituminous coal reserves in seams more than 14 inches thick." Coal seams in the Kootenai and Blackleaf Formations tend to be few, thin, and less-pure than the Morrison and were therefore not commercially mined.

Estimated Burial Depths

Overburden estimates based on sandstone properties followed the methods described in Klevberg and Oard (2023) and began with estimation of change in intergranular volume (IGV) or initial (matrix-free) porosity as summarized in Table III. The change in IGV was used to estimate compaction pressure from overburden using Bjørlykke's relation for reservoir sandstones (Bjørlykke, 2014). Results are included in Table IV along with estimated overburden using the methods outlined in Klevberg and Oard (2023).

1 U.S. coal is typically evaluated for heating value in terms of British thermal units per dry pound of coal (Btu/lb.).

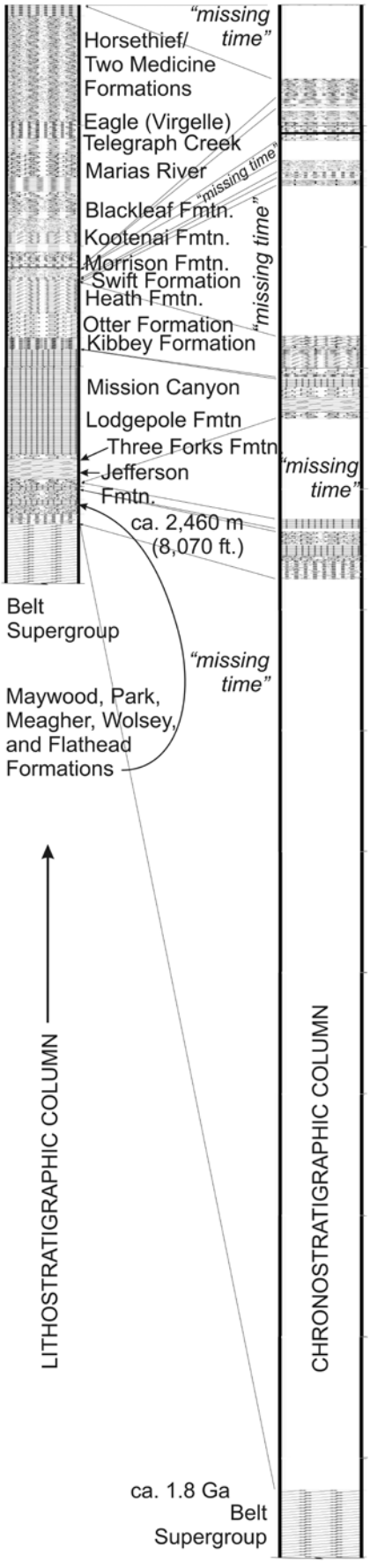

Figure 10 *(right)*. The left column is a lithostratigraphic column ("rock column") based on subcrop, and the right column is the geologic column ("time column") for the study area per Carstarphen et al. (2011). Notice how much of the alleged time has left no record in the rocks. Although some of these hiatuses show at least minor evidence of being unconformities, others show no such evidence.

Table II. Sample Properties

Sample	G008G	G008S	G008C	G008M
Geologic Unit	Flood Member, Blackleaf Formation	Sunburst Member, Kootenai Formation	Cut Bank Member, Kootenai Formation	Morrison Formation (uppermost unit)*
Classification	litharenite	sublitharenite	sublitharenite	litharenite
Sand Size	fine	fine	Fine	fine
Sorting	poor to moderate	poor	moderate to well	moderate to well
Grain Shape	angular–subangular	subangular	subangular	subangular–subrounded
Grain Size	0.2–1.9 mm	<5 µm–0.7 mm	0.1–0.3 mm	0.02–0.6 mm
Maturity	immature–submature	immature	submature–mature	immature–submature
Quartz	55–60%	80–85%	75–85%	55–60%
Feldspars	5–10%	1–2%	3–5%	5–10%
Lithic Fragments	30–35%	10–15%	10–15%	25–30%
Matrix, Cements	ca. 2% muscovite, glauconite, calcite	13–20% iron oxide with microquartz and phyllosilicates	<10% microquartz, phyllosilicates, calcite	25–35%, half iron oxide, balance microquartz, phyllosilicates
Opaque Minerals	3–5%		2–3%	
Pore Space	15–20%	5–15%	10–20%	5–15%
Comments	cross laminated; strained quartz, deformation twinning in mica	iron oxide is zoned; strained quartz	planar laminated; strained quartz	planar laminated; strained quartz

* Now more commonly classified as basal unit of Cut Bank Member, Kootenai Formation; superjacent to Morrison carbonaceous shale.

Table III. Estimates of Initial Porosity

Sample	Grain Size	Sorting	Shape	Matrix	Wet Sand	Porosity
G008C	49%	48%	45%	40%	35%	35%
G008G	49%	48%	45%	43%	38%	38%
G008M	49%	48%	46%	40%	35%	38%
G008S	49%	43%	40%	34%	25%	38%

Estimated Overburden

Overburden is proportional to burial depth, with the assumption that the average density of the overburden resembled typical density values of Kootenai and Blackleaf Formation strata. Table IV summarizes results from the three applicable methods for estimating overburden along with the method of Bjørlykke: estimates based on a graphical approach, local stratigraphic-section comparison (rock column based only

Figure 11. Sample G was collected from drill core obtained at the location shown in Figure 2 (47°29'05.85" North, 111°21'08.16" West). A is HQ core in tray. B is the section of core from which the sample was obtained, cut and lapped. C is thin section in plane polarized light. Arrows: 1 = detrital quartz, 2 = polycrystalline lithic fragments, 3 = feldspar, 4 = pore space. D is thin section in cross polarized light. The sample is a litharenite.

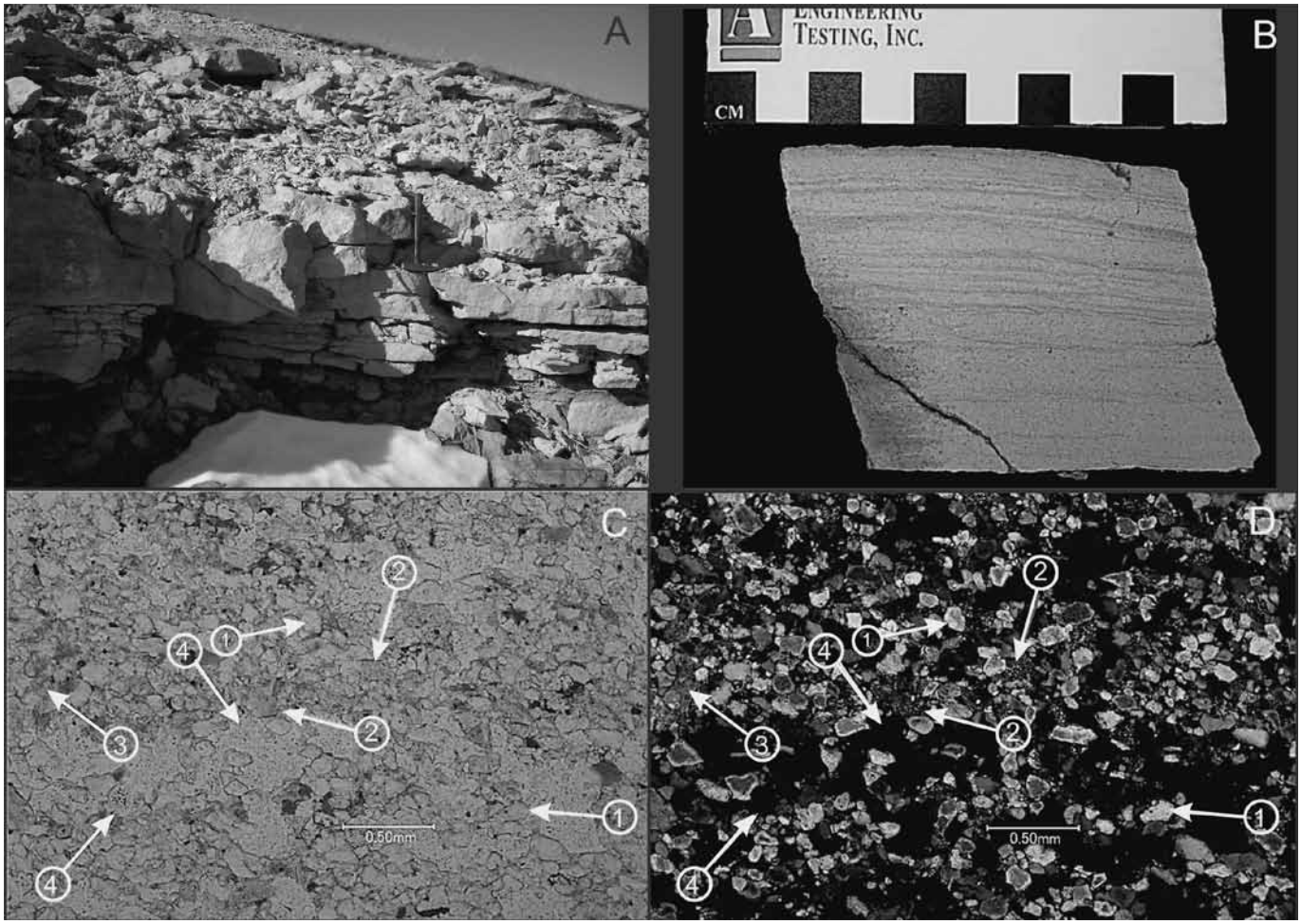

Figure 12. Sample C was collected at the location shown on Figure 2. A is fresh road cut north of Tracy (by Gerber, 47°26'46.12" North, 111°08'57.14" West) with rock pick at sample location of Cut Bank Sandstone. B is the sample as cut and lapped. C is thin section in plane polarized light. Arrows: 1 = detrital quartz, 2 = polycrystalline lithic fragments, 3 = calcite, 4 = pore space. D is thin section in cross polarized light. The sample is a sublitharenite.

on local outcrops), chronostratigraphic column (rock column plus presumed missing section from entire study area), and coal rank. The graphical approach provides a *minimum* overburden pressure based on Figures 6 and 7 compared with erosional remnants. The local stratigraphic section was derived from topographic maps and observed outcrops. It is also a *minimum* value as it does not account for earth materials eroded above the present land surface. The full stratigraphic section is based on both outcrop and subcrop in the study area as interpreted by Vuke et al. (2002) and Carstarphen et al. (2011). It is therefore more speculative than the local rock column, but probably still represents a minimum overburden thickness. Coal rank estimates are from Thomas (2013, p. 111).

Comparison of Results

The first three methods of estimated compaction pressure from overburden to infer burial depths are intended to provide minimum values, while the last two (Bjørlykke and coal rank) are intended to directly estimate depths using sandstone and coal properties, respectively. The minimum values are all less than the direct estimates as expected. However, the sandstone and coal rank methods differ markedly. The burial depth difference (based on the graphical method) between samples (115 m) is less than 2% of the average Bjørlykke depth estimate, so it may be neglected. Assuming a normal Gaussian distribution, the 95% confidence interval (±σ) is 2,800–9,800 m. The lower confidence limit

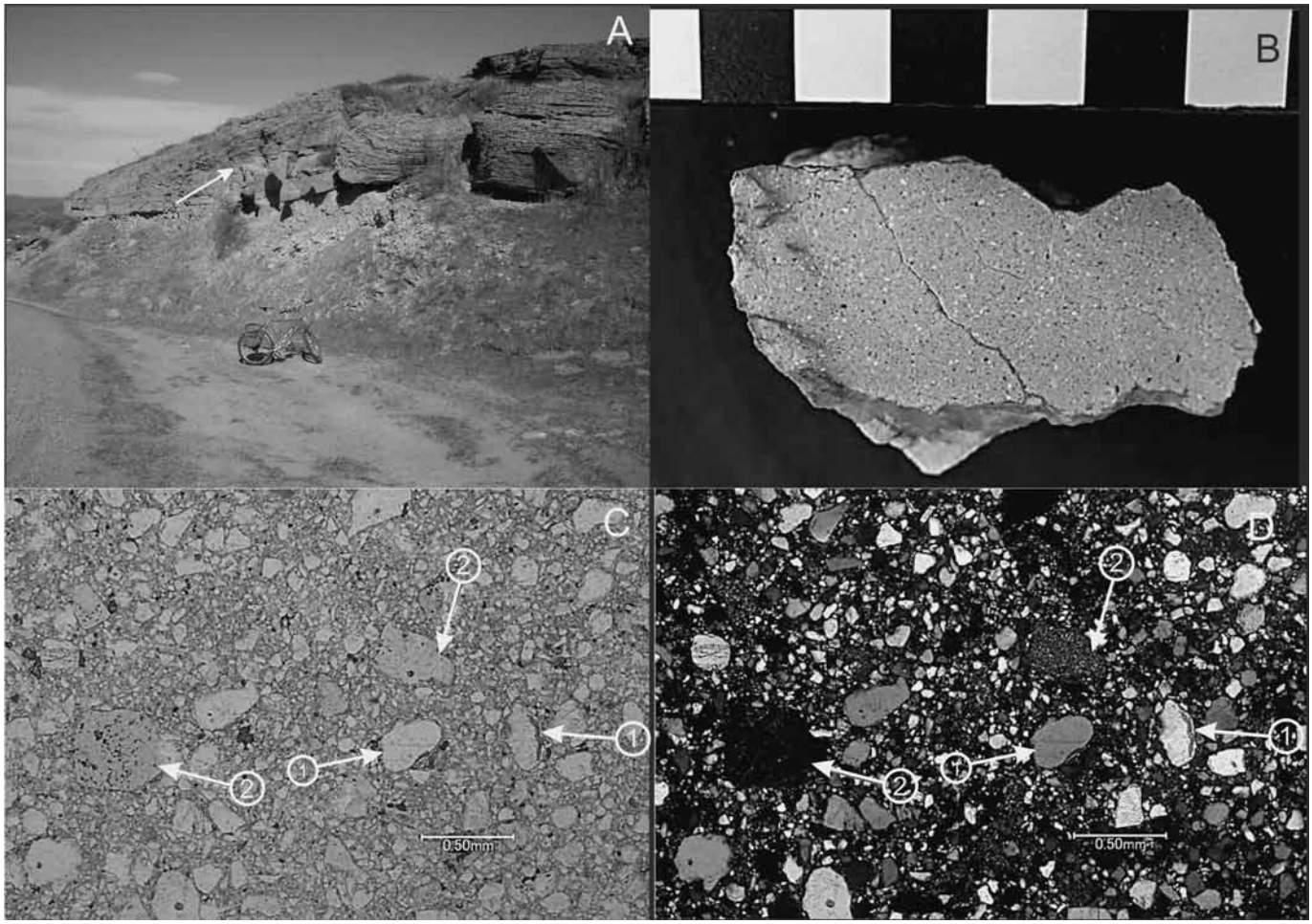

Figure 13. Sample S was collected at the location shown on Figure 2. A is Sunburst Sandstone Member outcrop east of Centerville (47°23'08.16" North, 111°07'27.49" West), view toward the west-northwest. Sample location indicated by arrow. B is the sample as cut and lapped. C is thin section in plane-polarized light. Arrows: 1 = detrital quartz, 2 = polycrystalline lithic fragments. D is thin section in cross-polarized light. The sample is a sublitharenite.

coincides with the lower limit of the coal rank estimated value; however, the mean using the Bjørlykke sandstone method is over twice the mean value using the coal rank method. There is a great deal of difference between the sandstone values, and they appear random relative to stratigraphic position. While some posit a minor unconformity between the Kootenai and Morrison Formations (Silverman and Harris, 1967), it would hardly accommodate 2,800 m of erosion between samples G008C and G008M per the Bjørlykke sandstone method. If the iron cement in sample G008M was deposited during mechanical compaction and thus interfered with it, then the estimated burial depth should be unrealistically low, not high.

Summary and Conclusions

Results may be summarized thusly:

1. Both Bjørlykke sandstone and coal rank methods indicate burial depths greater than the minima required by graphical and stratigraphic methods.
2. Variation in results using the sandstone methods is considerable, and the methods should be considered no better than order-of-magnitude estimates.
3. The coal rank coincided with the lower confidence limit of the sandstone method for the four samples in this study. It would be more conservative to use these results than the Bjørlykke sandstone results.
4. The sandstone results varied from each other at least an order of magnitude more than the actual vertical differences between samples (i.e.,

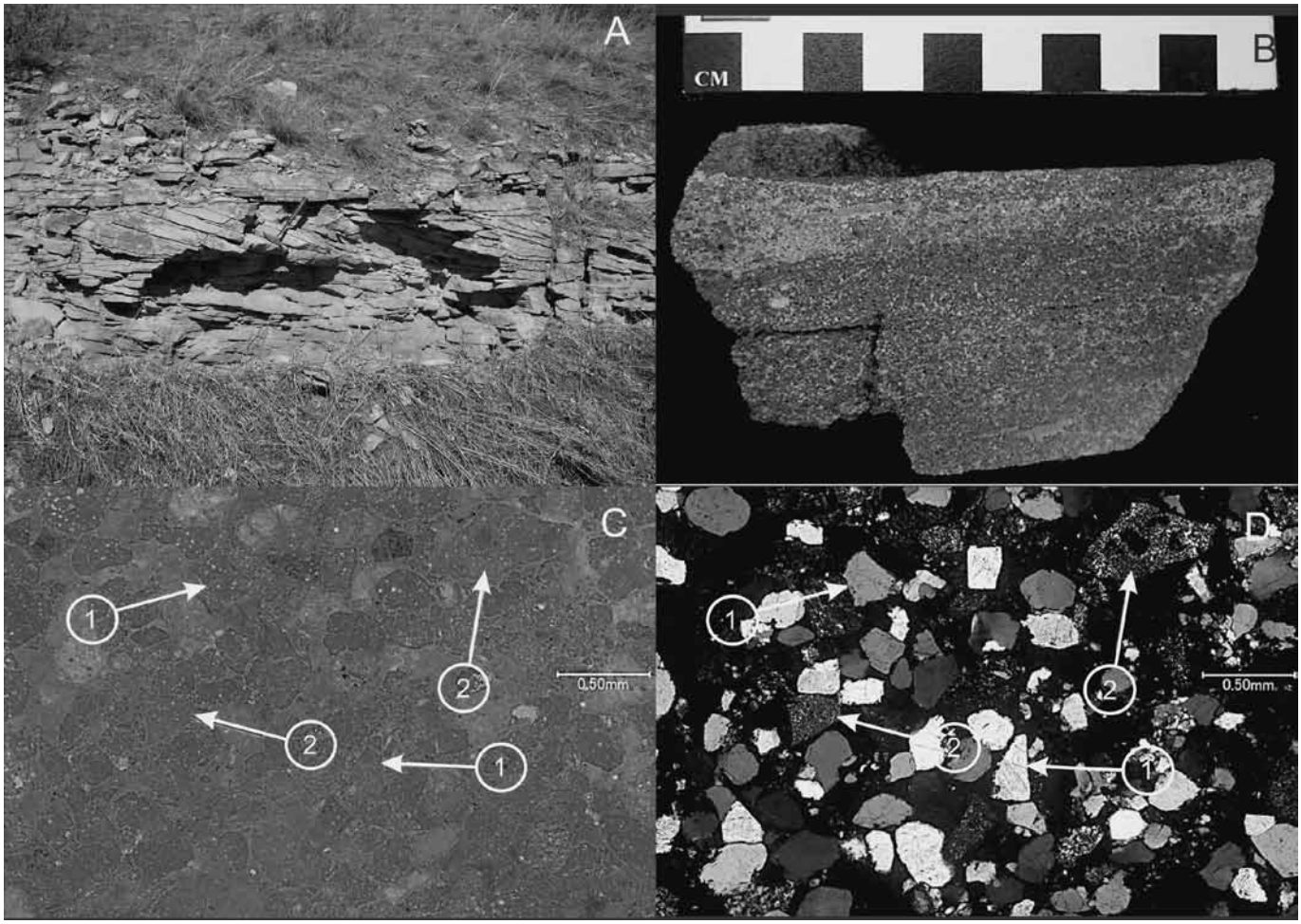

Figure 14. Sample M was collected at the location shown on Figure 2. A is sample location M west of Sand Coulee post office (47°23'57.44" North, 111°10'09.59" West), outcrop of medium-hard, medium-grained, thin-bedded and cross-bedded sandstone. Rock pick is at approximate location of sample. B is the sample as cut and lapped. C is thin section in plane polarized light. Arrows: 1 = detrital quartz, 2 = polycrystalline lithic fragments. D is a thin section in cross-polarized light. The sample is a litharenite.

Table IV. Estimated Overburden Thicknesses

	Sample			
Method	**G008G**	**G008S**	**G008C**	**G008M**
Graphical	375 m	425 m	480 m	490 m
Local Section	300 m	400 m	425 m	440 m
Full Section	1,050 m	1,150 m	1,175 m	1,190 m
Bjørlykke	5,600 m	4,800 m	6,000 m	8,800 m
Coal Rank	2,800-3,200 m	2,800-3,200 m	2,800-3,200 m	2,800-3,200 m

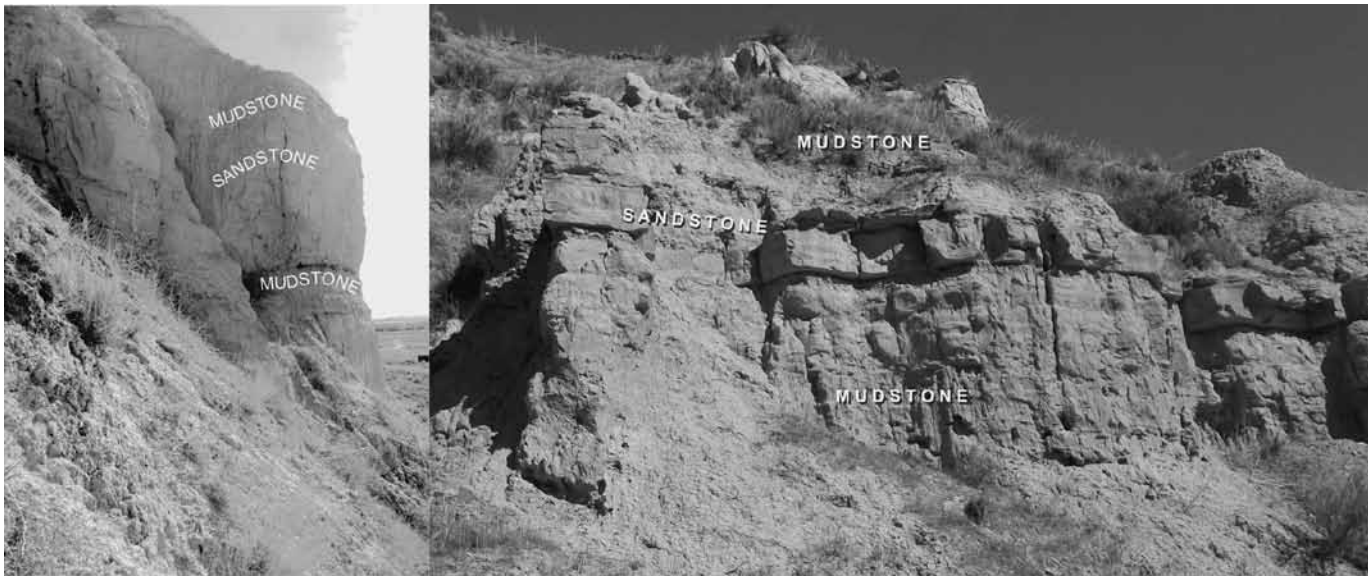

Figure 15. Fort Union strata near Broadus, Montana, containing lithified and unlithified intervals.

burial depth) would explain.

5. No vertical difference was indicated by coal rank since no difference in coal rank occurs over the limited vertical interval in the study area.
6. Lithologic differences between the samples are not reflected in any obvious pattern of compaction with depth.

In addition to the above, we draw the reader's attention to Figures 11 through 14. The presence of considerable angularity and lithic fragments in sandstones from four different units matches well with diluvial expectations of rapid physical weathering without much time for chemical weathering prior to deposition and diagenesis. It does not seem to match uniformitarian expectations of weathering horizons over vast ages of deposition and gradual lithification.

Inference of burial depth based on degree of lithification of sandstones is crude at best. Part of the explanation for this lies with the complexities of the sediments: grain size, sorting, angularity, mineralogy, grain coatings, matrix, etc. Another complicating factor is cementation, as explained more fully in Part I (Klevberg and Oard, 2023) and in Appendix A below. The importance of this can be illustrated in sedimentary sequences (Figure 15). While lithology can explain competent sandstone between poorly lithified mudstones, hard sandstones between poorly lithified sandstones are also common (Figure 13A). This clearly cannot result from compaction pressure. We may thus conclude that inference of burial depth can never be more than a crude approximation.

With or without precise means of burial-depth estimation, the need for a lithification model remains, and research will continue, especially for reservoir rocks. At this stage, we have only crude methods of obtaining initial estimates of maximum burial depth. We have at our disposal relatively accurate methods of estimating *minimum* overburden thickness (graphical from erosional remnants and local rock column), but these are of limited, local applicability. Equations of state and their time derivatives—i.e., rates of lithification-have yet to be developed. These will be far more complicated than mere overburden pressure.

As reported by the laboratory, compaction was evident in the samples (Table II and Braaten and Moulzolf, 2018, Appendix B). Evidence of compaction is often visible at the macroscopic scale, too, as in the contact between Kootenai and Morrison: "In most places the undulatory configuration of the base of the sandstone is due to compaction of the underlying shale and coal" (Silverman and Harris, 1967, p. 7). Bjørlykke's method, which is based on experimentation, is a step in the right direction, but it is still very crude based on the results of this study. Researchers should investigate whether reliance on popular modeling software with their uniformitarian assumptions for petroleum maturation may play a role in

the application of Bjørlykke's method. Because coal rank may have more to do with thermal history than pressure, it may make a better "thermometer" than burial-depth indicator.

More comprehensive lithification models are needed that include cementation (chemical compaction and chemical non-compaction) and that are independent of the kind of uniformitarian assumptions that hamstring basin models. These models can have import for reservoir analysis, geomechanical modeling, and analysis of diagenesis. However, they remain models and are beset by the inherent limitations of the modeling process. In the case of the sandstones proximate to the Great Falls Coal Field, we infer that the initial overburden contributing to the lithification of the four sampled units was probably more than 300 m (1,000 ft.) but likely less than 3,000 m (10,000 ft.). Until further research and refining of models is accomplished, these crude estimates are all that is possible, and confidence in more precise estimates is not warranted. Burial histories based on such inferences are subject to even greater potential error.

Acknowledgements

The laboratory work described in this paper was supported by a grant from the Creation Research Society. *Deum laudamus* (Job 28:5).

References

Anderson, P. No Date. Giffen Mine. *Historic American Engineering Record, Report HAER No. MT-30*. Rocky Mountain Regional Office, National Park Service, Denver, CO.

Barrick, W.D. 2018. Exegetical analysis of Psalm 104:8 and its possible implications for interpreting the geologic record. In Whitmore, J.H. (editor). *Proceedings of the Eight International Conference on Creationism*, pp. 95–102. Creation Science Fellowship, Pittsburgh, PA.

Barrick, W.D., M.J. Oard, and P. Price. 2020. Psalm 104:6–9 likely refers to Noah's Flood. *Journal of Creation* 34(1): 102–109.

Bjørlykke, K. 2014. Relationships between depositional environments, burial history and rock properties. Some principal aspects of diagenetic process [sic] in sedimentary basins. *Sedimentary Geology* 301: 1–14.

Bjørlykke, K., and J. Jahren. 2018. Open or closed geochemical systems during diagenesis in sedimentary basins: Constraints on mass transfer during diagenesis and the prediction of porosity in sandstone and carbonate reservoirs. *AAPG Bulletin* 96(12): 2193–2214.

Braaten, C.J., and G. Moulzolf. 2018. Material Check. *American Engineering Testing Project No. 24–20180*. American Engineering Testing, Inc., Saint Paul, MN. (Included herein as Appendix B.)

Carstarphen, C.A., L.N. Smith, D.C. Mason, J.I. LaFave, and M.G. Richter. 2011. Data for water wells visited during the Cascade–Teton Groundwater Characterization Study. *Montana Groundwater Assessment Atlas 7B*. Montana Bureau of Mines and Geology, Butte, MT.

Chuhan, F.A., A. Kjeidstad, K. Bjørlykke, and K. Høeg. 2002. Porosity loss in sand by grain crushing—experimental evidence and relevance to reservoir quality. *Marine and Petroleum Geology* 19(1): 39–53.

Cui, Y., S.J. Jones, C. Saville, S. Stricker, G. Wang, L. Tang, X. Fan, and J. Chen. 2017. The role played by carbonate cementation in controlling reservoir quality of the Triassic Skagerrak Formation, Norway. *Marine and Petroleum Geology* 85: 316–331.

Fawad, M., N.H. Mondol, J. Jahren, and K. Bjørlykke. 2011. Mechanical compaction and ultrasonic velocity of sands with different texture and mineralogical composition. *Geophysical Prospecting* 59(4): 697–720.

Fisher, C.A. 1909. Geology of the Great Falls Coal Field, Montana. *U.S. Geological Survey Bulletin* 356. U.S. Government Printing Office, Washington, D.C.

Klevberg, P. and M.J. Oard. 2023. Lithification of sediments—Part I: Significance, processes, and modeling. *CRSQ* 60(1): 11–28.

Klevberg, P., and M.J. Oard. 1998. Paleohydrology of the Cypress Hills Formation and Flaxville Gravel. In Walsh, Robert E. (editor). *Proceedings of the Fourth International Conference on Creationism*, pp. 581–592. Creation Science Fellowship, Pittsburgh, PA.

Li, Y., X. Chang, W. Yin, T. Sun, and T. Song. 2017. Quantitative impact of diagenesis on reservoir quality of the Triassic Chang 6 tight oil sandstones, Zhenjing area, Ordos Basin, China. *Marine and Petroleum Geology* 86:1014–1028.

Monsees, A.C., Busch, B., Schöner, N., and Hilgers, C. 2020. Rock typing of diagenetically induced heterogeneities—a case study from a deeply-buried clastic Rotliegend reservoir of the Northern German Basin. *Marine and Petroleum Geology* 113(104163): 1–14.

Neuendorf, K.K., J.P. Mehl, Jr., and J.A. Jackson. 2005. *Glossary of Geology*, Fifth edition. American Geological Institute, Alexandria, VA.

Oard, M.J. 2008. *Flood by Design: Receding Water Shapes the Earth's Surface*. Master Books, Green Forest, AR.

Oard, M.J. ebook. 2013. *Earth's Surface Shaped by Genesis Flood Runoff*; http://Michael.oards.net/GenesisFloodRunoff.htm.

Oard, M.J., and P. Klevberg. 1998. A diluvial interpretation of the Cypress Hills Formation, Flaxville gravel, and related deposits. In Walsh, Robert E. (editor). *Proceedings of the Fourth International Conference on Creationism*, pp. 421–436. Creation Science Fellowship. Pittsburgh, PA.

Prajapati, N., A.A. Bonzalez, M. Selzer, B. Nestler, B. Busch, and C. Hilgers. 2020. Quartz cementation in polycrystalline sandstone: Insights from phase-field simulations. *Journal of Geophysical Research: Solid Earth* 125(2):

e2019JB019137.

Rossillon, M., M. McCormick, and M. Hufstetler. 2009. *Great Falls Coal Field: Historic Overview*. Renewable Technologies, Inc., Butte, MT.

Silverman, A.J., and W.L. Harris. 1967. Stratigraphy and economic geology of the Great Falls–Lewistown Coal Field, Central Montana. *Montana Bureau of Mines and Geology Bulletin 56*. Montana Bureau of Mines and Geology, Butte, MT.

Thomas, L. 2013. *Coal Geology*, Second edition. Wiley-Blackwell, Chichester, West Sussex, UK.

Vuke, S.M. 2000. *Geologic Map of the Great Falls South 30' x 60' Quadrangle, Central Montana*. Montana Bureau of Mines and Geology Open File 407. Montana Bureau of Mines and Geology, Butte, MT.

Vuke, S.M., R.B. Colton, and D.S. Fullerton. 2002. *Geologic Map of the Great Falls North 30' x 60' Quadrangle, Central Montana*. Montana Bureau of Mines and Geology Open File 459. Montana Bureau of Mines and Geology, Butte, MT.

Walker, T. 1994. A Biblical geological model. In Walsh, R.E. (editor). *Proceedings of the Third International Conference on Creationism*, technical symposium sessions, pp. 581–592. Creation Science Fellowship, Pittsburgh, PA; biblicalgeology.net/.

Xia, L., Z. Liu, Y. Cao, W. Zhang, J. Liu, C. Yu, and Y. Hou. 2020. Postaccumulation sandstone porosity evolution by mechanical compaction and the effect on gas saturation: Case study of the Lower Shihezi Formation in the Bayan'aobao area, Ordos Basin, China. *Marine and Petroleum Geology* 115(104253): 1–16.

Appendix A

Sedimentary rocks present questions for diluvialists as well as uniformitarian scientists. Once sediments accumulate, they need to be cemented to become sedimentary rocks. Compaction is only one mechanism contributing to lithification. We commonly see sedimentary rocks on the surface, and sequences of various types of sedimentary rocks in cliffs that are almost always cemented. How did they lithify? Was it during the Deluge? Were near-surface sediments cemented after the Genesis Flood? Or can it be both?

Cementation, related to the porosity and permeability, is a complicated process that depends upon numerous variables that have not been completely worked out: "As a result, porosity reducing processes need to be understood in order to evaluate and model [oil] reservoir quality in sandstones" (Monsees et al., 2020, p. 1). Xia et al. (2020, p. 2) state: "In fact, the process of porosity evolution caused by post-accumulation compaction in sandstone reservoirs remains poorly understood." Porosity is the percentage of the bulk volume of a rock, sediment, or soil that is occupied by air or fluid, whether isolated or connected (Neuendorf et al., 2005, p. 508). Permeability is different and is defined as the property or capacity of a porous rock, sediment, or soil for transmitting a fluid (Neuendorf et al., 2005, p. 483). Permeability can vary a lot with any particular porosity, but in general permeability of sandstones is an exponential function of porosity (Li et al., 2017).

Cementation depends upon the type of sediment deposited, such as sand, mud, carbonate, or combinations of these three. It also depends upon the character of the detrital or framework grains, such as the size, sorting, angularity, mineralogy, the amount and composition of matrix within the sediment, etc. (Bjørlykke, 2014). Sorting refers to the uniformity of the sizes of the grains (Neuendorf et al., 2005, p. 613). The framework or detrital grains are the main grains that make up the sediment, for instance quartz sand in a sandstone. Some sandstones like quartz arenite have greater than 90–95% quartz grains. But other sandstones may also be high in feldspar and rock particles that significantly affect cementation.

Besides the framework grains, the sandstone not only has voids, it also has smaller matrix particles between grains that make cementation even more complicated. The sum of voids, matrix particles, and cement is called the *intergranular volume* (IGV) (Cui et al., 2017).

During and after a sediment accumulates, diagenetic and authigenetic processes change the sediment, one of these processes being cementation. Diagenesis is the sum of all physical and chemical changes in minerals during and after their initial accumulation (Neuendorf et al., 2005, p. 176). Authigenesis is a little different. It refers to the processes by which *new* minerals form within a sediment or sedimentary rock during or after deposition, such as recrystallization or cementation (Neuendorf et al., 2005, p. 44).

Appendix B

See A.E.T. report, pp. 316–319.

Appendix C

See Table of Stratigraphy of Study Area, p. 320.

Appendix B: AET report, p. 1

24-LAB-004
PETROGRAPHIC EXAMINATION OF ROCK, ASTM C295

AET JOB NO: 24-20180 **DATE:** 9-18-2018
SAMPLE ID: G008 C **PETROGRAPHER:** C. Braaten

DESCRIPTION:
The rock was classified as a sublitharenite, fine grained sandstone. The rock was poorly cemented and generally consisted of sand sized quartz and lithic particles. The rock used for analysis was a cross section, which was laboratory sawcut from the original sample. The original dimensions of the rock were approximately 102 mm (4") x 76 mm (3") x 51 mm (2") thick. The selected sawcut section of rock was approximately 83 mm (3-1/4") x 68 mm (2-11/16") x 34 mm (1-5/16") thick. A thin section was also produced from the other cross section of the rock. The rock was contained alternating laminations which were similar to yellowish gray and medium gray (Munsell® 5Y 8/1 and N5) in color. Thin section and hand sample of the rock were used for the rock description. The sample used for thin section was impregnated with an optically clear epoxy to aid in sample stabilization.

In hand sample, the rock was relatively soft and friable. The rock also appeared to be "fresh" and unweathered. A Mohs hardness pick of 3 produced a scratch and liberated grains from the rock. The hand sample appeared relatively absorptive as a water bead dispersed into the stone within several seconds. The rock contained numerous, relatively parallel, laminations. These laminations generally alternated between yellowish gray and medium gray. The yellowish gray layers ranged in thickness from approximately 1 mm up to 8 mm and the medium gray layers ranged from approximately 0.5 mm up to 2 mm in thickness. The yellowish gray layers were dominant within the rock. A few fractures were also observed within the rock.

In thin section, sand-sized quartz and lithic particles were the major constituents observed within the rock. The grains were chiefly sub-angular and moderately to well sorted. Combining these two textures classifies the rock as submature to mature sandstone. Grains ranged in size from approximately 0.01 mm up to 0.3 mm. Quartz was observed as monocrystalline grains and polycrystalline within lithic particles. Several quartz grains exhibit undulose extinction (straining). Lithic particles comprised approximately 10-15% of the rock. Quartz and feldspar minerals comprised the rest of the detrital grains, where feldspar was approximately 3-5% and quartz was approximately 75-85%. Pore space was difficult to estimate due to difficulty in thin section preparation; however, it appeared to be approximately 10-20%. The lithic particles consisted of chert and polycrystalline quartz. Cryptocrystalline mineral material was observed as cement/matrix within zones of the rock. The cryptocrystalline mineral material appeared "dusty" and was most likely comprised of micas, quartz, and/or clay minerals. Small amounts of carbonate cement were observed in a patchy nature throughout the rock. A few opaque materials were observed within the rock. These opaques did not exhibit a metallic luster and may be organic material or oxides.

MINERALOGY:		OPTICAL PROPERTIES:			
MINERALS	VOL(%)*	COLOR	BIREFRINGENCE	RELIEF	OTHER
quartz	80 – 85	colorless	low 1st order	low	detrital grains and within lithic particles
feldspar	3 – 5	colorless	low 1st order	low	detrital grains
muscovite	trace	colorless	2nd order	moderate	detrital grains
biotite	trace	pleo. green/brown	3rd to 4th order, masked	moderate	detrital grains
calcite	1 – 2	colorless	high 3rd to 4th order	variable	patchy zones of cement
opaques	2 – 3	opaque	--	--	brown to black in reflected light
cryptocrystalline material	< 10	colorless to "dusty" brown	--	--	cement/matrix material, possibly micas, quartz, and/or clay minerals
iron-oxide	2 – 3	opaque	--	--	reddish brown in reflected light

* Based on visual estimation of thin section

Appendix B: AET report, p. 2

24-LAB-004
PETROGRAPHIC EXAMINATION OF ROCK, ASTM C295

AET JOB NO: 24-20180 **DATE:** 9-18-2018
SAMPLE ID: G008 G **PETROGRAPHER:** C. Braaten

DESCRIPTION:
The rock was classified as a litharenite, fine grained sandstone. The rock was poorly cemented and generally consisted of sand sized quartz and lithic particles. The rock used for analysis was a cross section, which was laboratory sawcut from the original sample. The original dimensions of the rock core were approximately 76 mm (3") diameter x 44 mm (1-3/4") long. The selected sawcut section of rock was approximately 73 mm (2-7/8") x 42 mm (1-5/8") x 30 mm (1-3/16") thick. A thin section was also produced from the other cross section of the rock. The rock contained alternating zones which were similar to very light gray to light gray and medium dark gray (Munsell® N8 to N7 and N4) in color. Thin section and hand sample of the rock were used for the rock description. The sample used for thin section was impregnated with an optically clear epoxy to aid in sample stabilization.

In hand sample, the rock was relatively soft and friable. The rock also appeared to be "fresh" and unweathered. A Mohs hardness pick of 3 produced a scratch and liberated grains from the rock. The hand sample appeared relatively absorptive as a water bead dispersed into the stone within several seconds. The rock contained numerous, irregularly oriented seams (cross laminations?) of different color.

In thin section, sand-sized quartz and lithic particles were the major constituents observed within the rock. The grains were chiefly angular to sub-angular and poorly to moderately sorted. Combining these two textures classifies the rock as immature to submature sandstone. Grains ranged in size from approximately 0.02 mm up to 1.9 mm. Quartz was observed as monocrystalline grains and polycrystalline within lithic particles. Several quartz grains exhibit undulose extinction (straining). Lithic particles comprised approximately 30-35% of the rock. Quartz and feldspar minerals comprised the rest of the detrital grains, where feldspar was approximately 5-10% and quartz was approximately 55-60%. Pore space was approximately 15-20%. The lithic particles consisted of chert, siltstone, and polycrystalline quartz. Small amounts of carbonate cement were observed in a patchy nature throughout the rock. Deformation twinning was observed within a few mica particles. A few opaque materials were observed within the rock. These opaques did not exhibit a metallic luster and may be organic material or oxides.

MINERALOGY:		OPTICAL PROPERTIES:			
MINERALS	VOL(%)*	COLOR	BIREFRINGENCE	RELIEF	OTHER
quartz	85 – 90	colorless	low 1st order	low	detrital grains and within lithic particles
feldspar	5 – 10	colorless	low 1st order	low	detrital grains
muscovite	trace	colorless	2nd order	moderate	detrital grains
glauconite	trace	pale green	anomalous	low	detrital grain
calcite	1 – 2	colorless	high 3rd to 4th order	variable	patchy zones of cement
opaques	3 – 5	opaque	--	--	brown to black in reflected light

* Based on visual estimation of thin section

Appendix B: AET report, p. 3

24-LAB-004
PETROGRAPHIC EXAMINATION OF ROCK, ASTM C295

AET JOB NO: 24-20180 **DATE:** 9-18-2018
SAMPLE ID: G008 M **PETROGRAPHER:** C. Braaten

DESCRIPTION:
The rock was classified as a litharenite, fine grained sandstone. The rock was poorly cemented and generally consisted of sand sized quartz and lithic particles. The rock used for analysis was a cross section, which was laboratory sawcut from the original sample. The original dimensions of the rock were approximately 95 mm (3-3/4") x 76 mm (3") x 44 mm (1-3/4") thick. The selected sawcut section of rock was approximately 92 mm (3-5/8") x 45 mm (1-3/4") x 33 mm (1-5/16") thick. A thin section was also produced from the other cross section of the rock. The rock contained alternating laminations which were similar to pale yellowish brown and grayish orange to light brown (Munsell® 10YR 6/2 and 10YR 6/6 to 5YR 5/6) in color. Thin section and hand sample of the rock were used for the rock description. The sample used for thin section was impregnated with an optically clear epoxy to aid in sample stabilization.

In hand sample, the rock was relatively soft and friable. The rock also appeared to be "fresh" and unweathered. A Mohs hardness pick of 3 produced a scratch and liberated grains from the rock. The hand sample appeared relatively absorptive as a water bead dispersed into the stone within several seconds. The rock contained generally sub-parallel to parallel laminations. The laminations alternated in color between pale yellowish brown and grayish orange to light brown. The grayish orange to light brown laminations contained iron oxide cement.

In thin section, sand-sized quartz and lithic particles were the major constituents observed within the rock. The grains were chiefly sub-rounded to sub-angular and moderately to well sorted. Combining these two textures classifies the rock as immature to submature sandstone. Grains ranged in size from approximately 0.02 mm up to 0.6 mm. Quartz was observed as monocrystalline grains and polycrystalline within lithic particles. Several quartz grains exhibit undulose extinction (straining). Lithic particles comprised approximately 25-30% of the rock. Quartz and feldspar minerals comprised the rest of the detrital grains, where feldspar was approximately 5-10% and quartz was approximately 60-65%. Pore space was approximately 5-15%. The lithic particles consisted of chert, siltstone, shale, and polycrystalline quartz. Several detrital quartz grains appeared to have syntaxial rims of quartz. Iron oxide was observed as a cement within a few of the laminations and cryptocrystalline mineral material was observed as the cement/matrix within the other laminations. The cryptocrystalline mineral material appeared "dusty" and was most likely comprised of micas, quartz, and/or clay minerals.

MINERALOGY:		OPTICAL PROPERTIES:			
MINERALS	VOL(%)*	COLOR	BIREFRINGENCE	RELIEF	OTHER
quartz	55 – 60	colorless	low 1st order	low	detrital grains and within lithic particles
feldspar	5 – 10	colorless	low 1st order	low	detrital grains
amphibole	trace	pleo. green	2nd order, masked	moderate to high	detrital grains
biotite	trace	pleo. green/brown	3rd to 4th order, masked	moderate	detrital grains
cryptocrystalline material	10 – 15	colorless to "dusty" brown	--	--	cement/matrix material, possibly micas, quartz, and/or clay minerals
iron-oxide	15 – 20	opaque	--	--	reddish brown in reflected light

* Based on visual estimation of thin section

Appendix B: AET report, p. 4

24-LAB-004
PETROGRAPHIC EXAMINATION OF ROCK, ASTM C295

AET JOB NO: 24-20180 **DATE:** 9-18-2018
SAMPLE ID: G008 S **PETROGRAPHER:** C. Braaten

DESCRIPTION:
The rock was classified as a sublitharenite, fine grained sandstone. The rock was poorly cemented and generally consisted of sand sized quartz and lithic particles. The rock used for analysis was a cross section, which was laboratory sawcut from the original sample. The original dimensions of the rock were approximately 76 mm (3") x 64 mm (2-1/2") x 44 mm (1-3/4") thick. The selected sawcut section of rock was approximately 60 mm (2-3/8") x 45 mm (1-3/4") x 28 mm (1-1/8") thick. A thin section was also produced from the other cross section of the rock. The rock was similar to yellowish gray (Munsell® 5Y 8/1) in color with a few dark yellowish orange (Munsell® 10YR 6/6) zones. Thin section and hand sample of the rock were used for the rock description. The sample used for thin section was impregnated with an optically clear epoxy to aid in sample stabilization.

In hand sample, the rock was relatively soft and friable. The rock also appeared to be "fresh" and unweathered. A Mohs hardness pick of 3 produced a scratch and liberated grains from the rock. The hand sample appeared relatively absorptive as a water bead dispersed into the stone within several seconds. Several micro-fractures were observed within the rock. A few zones within iron oxide cement were also observed.

In thin section, sand-sized quartz and lithic particles were the major constituents observed within the rock. The grains were chiefly sub-angular to angular and poorly sorted. Combining these two textures classifies the rock as immature sandstone. Grains ranged in size from approximately < 5 µm up to 0.7 mm. Quartz was observed as monocrystalline grains and polycrystalline within lithic particles. Several quartz grains exhibit undulose extinction (straining). Lithic particles comprised approximately 10-15% of the rock. Quartz and feldspar minerals comprised the rest of the detrital grains, where feldspar was approximately 1-2% and quartz was approximately 85-90%. Pore space was approximately 5-15%. The lithic particles consisted of chert and polycrystalline quartz. Cryptocrystalline mineral material was observed as the cement/matrix within rock. The cryptocrystalline mineral material appeared "dusty" and was most likely comprised of micas, quartz, and/or clay minerals. Iron oxide was observed as a cement within a few zones within the rock.

MINERALOGY:		OPTICAL PROPERTIES:			
MINERALS	VOL(%)*	COLOR	BIREFRINGENCE	RELIEF	OTHER
quartz	80 – 85	colorless	low 1st order	low	detrital grains and within lithic particles
feldspar	1 – 2	colorless	low 1st order	low	detrital grains
amphibole	trace	pleo. green	2nd order, masked	moderate to high	detrital grains
zircon	trace	colorless	high 3rd to 4th order	very high	detrital grains
cryptocrystalline material	10 – 15	colorless to "dusty" brown	--	--	cement/matrix material, possibly micas, quartz, and/or clay minerals
iron-oxide	3 – 5	opaque	--	--	reddish brown in reflected light

* Based on visual estimation of thin section

Appendix C—Stratigraphy of Study Area

Group	Formation	Member	Lithologies (Vuke, 2000; Vuke et al., 2002)
Montana	Telegraph Creek		Very fine to fine grained calcareous sandstone interbedded with silty mudstone, fissile shale: 150–330 ft.
Colorado	Marias River	Kevin	Intimately interbedded, concretionary limestone, shaly very fine grained sandstone; middle unit has numerous beds ironstone concretions, concretionary limestone and dolostone, discontinuous conglomerate; thin bentonite beds, calcareous concretions in basal unit: 0–700 ft.
		Ferdig	Hard shale, few thin beds limestone concretions, hackly limestone; in middle unit, very fine grained, wavy/lenticular bedded sandstone/siltstone w/trace fossils, numerous flakes iron stained siltstone; few fine grained sandstone stringers, ferruginous dolostone and limestone concretions in basal unit: 100–200 ft.
		Cone	Calcareous/silty shale w/white specks, fish scales, petroliferous, interbedded w/thin, silty, irregulaly bedded crystalline limestone, over argillaceous, shaly, platy limestone, over calcareous/noncalcareous shale w/bentonite bed, zone septarian limestone concretions; basal limonitic siltstone, fish teeth and bones: 50–65 ft.
		Floweree	Noncalcareous shale, silty shale w/thin beds fine grained sandstone and siltstone, concretions: 10–35 ft.
	Blackleaf	Bootlegger	Relatively well cemented thin beds of sandstone and siltstone interbedded with silty shale and several bentonite beds; fish scales on some bedding planes; many places coarse grained, well cemented sandstone or pebble conglomerate at top w/fish scales, bones; two basal fine-medium grained sandstone units: 150–330 ft.
		Vaughn	Colorful, very bentonitic claystone interbedded with thinner lenticular bentonitic siltstone, sandstone, tuffaceous, porcellanitic; clinoptilolite, carbonaceous shale beds, some coal, basal medium grained arkosic sandstone: 52–86 ft.
		Taft Hill	Bentonitic siltstone, bentonitic shale, bentonite beds, over fine to medium grained, glauconitic sandstone; lower dominantly poorly to moderately fissile shale w/siltstone, fine grained sandstone, thin bentonite beds: 242–249 ft.
		Flood	Fine to medium grained, relatively resistant sandstone, siltstone, some granule conglomerate, coarse sandstone, carbonaceous shale, zone of calcareous sandstone concretions, over shale, siltstone, sandstone w/trace fossils. Sandstone west, shale east: ca. 140 ft.
	Kootenai	Kk5	Red weathering mudstone w/lenses, beds cross bedded, micaceous sandstone, nodular limestone concretions. Lower unit shale, lignite: ca. 230 ft.
		Kk4	Limestone, interbedded shale, fossiliferous, over fine to medium grained, platy, thin to medium bedded sandstone, mudstone interbeds; channels with fill ranging from mudstone to sandstone, interbedded, overlying or cutting through the Sunburst Sandstone, locally resting on the Cutbank Sandstone (Hopkins, 1985; Schwartz, personal communication, 2002). Channel fill fine to coarse grained, biotitic, lithic sandstone with steep forsets and sparse associated coal stringers: up to 200 ft.
		Sunburst	Well sorted, well cemented, resistant quartz sandstone, limonite specks, cross bedding, ripple lamination, trace fossils near top: 50 ft.
		Kk2	Dark gray mudstone grading downward into red mudstone: 0–100 ft.
		Cut Bank	Moderately well sorted, coarse to fine grained, festoon cross bedded, quartzose sandstone, fining upward, chert, discontinuous basal chert conglomerate: 0.1–100 ft.
	Morrison		Weathered mudstone w/interbedded micrite lenses, fine to medium grained, calcareous, thin bedded, sandstone like underlying Swift Formation, subbituminous coal / carbonaceous shale bed ≤12 ft. thick near top; gradational contacts w/Swift, Kootenai, but significant intraformational unconformity: 86–166 ft.

Bolded names indicate units sampled in this study.